PHYSICAL REVIEW B VOLUME 27, NUMBER 6 15 MARCH 1983

Eigenvalues of two-dimensional harmonic systems with periodic structures

Chia C. Shih
Department of Physics and Astronomy, University of Tennessee, Knoxville, Tennessee 37996-1200
(Received 11 March 1981; revised manuscript received 18 August 1982)

A recent technique of amplitude analysis for one-dimensional systems is generalized to a class of two-dimensional harmonic systems with nearest-neighbor interaction and periodic structures. The characteristic equation for the eigenvalues is reduced to a set of polynomial equations of order equal to the number of particles in the unit cell for finite and infinite crystals. Most of the analytic solutions demonstrated cannot be readily obtained by other methods. Numerical examples of precise eigenvalues and eigenvectors for some large but finite lattices (15×12, 15×21) can also be evaluated very accurately and efficiently. Analytic and numerical examples of several infinite strips are presented using both the fixed-end and cyclic-boundary conditions.

I. INTRODUCTION

Recently a new technique was developed to analyze the eigenvalue problem in one-dimensional linear systems with periodic structures.[1] A set of low-order polynomial equations specified completely by the structure of the unit cell has been constructed to replace the overall high-order characteristic determinant. Eigenproperties previously difficult to perceive can be analyzed. It is natural to consider generalizing this formalism beyond one-dimension analysis where traditional methods are limited.

Higher-dimensional systems are intrinsically rather involved, both numerically and analytically. As a consequence, explicit expressions for eigenvalues and eigenvectors of finite systems and the density of states (DOS) of infinite systems are not reported extensively in the literature. For infinite systems, an elegant example of the DOS for the multidimensional simple "cubic" lattice can be found in an early work by Montroll.[2] Starting from the fundamental work of Van Hove,[3] various analyses of the singularity structures of DOS have also been performed for homogeneous crystals. Recently, Dy, Wu, and Spratlin[4] succeeded in generalizing the sequential Green's-function method to a block-diagonal form. Surface effects on the DOS can then be treated analytically. It is, nevertheless, not possible to apply these existing methods directly to mixed crystals with complicated structures.

In principle, as long as the unit cells of an infinite crystal exhibit displacement symmetry between each other, a Bloch theorem should be imposed.[5] However, a simple adoption of the Bloch theorem would require the labeling of every element in the unit cell. This can become impractical when the cell structure is complicated, or when the concentration of any species becomes low.[5] For example, a structure of $\binom{BABB}{AAAA}\cdots)$ would require 6×6 matrices, and a 1% concentration of B would require 100×100 matrices. Neither the examination of the characteristic equation nor the expansion of the sequential Green's function is useful when attempting to take into account the full structure of the unit cell. It is therefore necessary to study the analytic structure of the eigenvectors within a unit cell and their propagation across the boundary between cells.

For finite systems with periodic structures, Hari used a transfer matrix method in 1968 and studied several simple physical systems.[6] These included one isotropic impurity at a single site, a whole-line impurity, and an impurity on the boundary. There have been very few further studies in this direction.[7] Besides analytic studies, nearly all numerical analysis has been performed on finite systems. Both large matrices and very-high-precision calculations are often needed. Various techniques have been developed to overcome these limitations. For example, the classical negative eigenvalue counting method of Dean[8,9] counts the number of normal modes in a given frequency interval without evaluating specific eigenvectors. The effective-medium sequential Green's-function method of Wu[10] starts from a small number of near neighbors and progressively expands the boundary. Both methods are attractive in disordered systems where periodic structures are absent. There is, however, no natural way to impose symmetry explicitly, or to avoid repeated identical calculation. Furthermore, as the size of a system increases, an accurate evaluation of any single eigenvalue is very time consuming. This makes an evaluation of the associated eigenvectors even

more difficult. The nearly singular secular equation requires extreme care in order to project the eigenvectors without systematic errors.[11,12]

Usually in the past, finite systems have been used to understand the behavior of infinite systems which can be approximately truncated in size. However, recent advances in submicrometer physics and biophysics are beginning to call attention to periodic structures of finite microscopic extension. In these systems, the boundary conditions may not be ignorable. In other words, without displacement symmetry, the Bloch theorem is no longer applicable. Detailed analysis of finite but large periodic systems is therefore increasingly desirable for its own sake.

The work we report here is a first attempt to address this problem. Instead of examining individual atoms, propagation and coupling of standing waves are employed. By generalizing the previous formulation of one-dimensional systems, the structure of a "modulating matrix" which summarizes the propagation of a standing wave across the boundary of a unit cell can be analyzed. Factorization of the characteristic equation can then be obtained even for finite systems without evoking a Bloch-type argument. The evaluation of the eigenvalues and eigenvectors for a mixed system can be sufficiently simplified to allow accurate numerical calculations. These modulation matrices also provide a convenient ingredient in imposing Bloch properties on an infinite or cyclic crystal.

In our formulation, the concluding relationship that governs the standing-wave patterns are usually simple. However, notations and intermediate relationships are often tedious. This reflects the intrinsic complexity of mixed crystals in general, and cannot be completely avoided. Details of the steps not essential to the flow of the derivation are therefore deferred to an Appendix. In Sec. II we briefly review the notation and the dynamical equations. In Sec. III solutions corresponding to several kinds of *finite but large* mixed crystals are worked out in more detail. This enables us to demonstrate the general approach without going into the full generality. A straightforward numerical calculation with good accuracy, using traditional methods, is nearly impossible in these cases. Section III also demonstrates, among other properties, the factorization of the characteristic equations. The analytic solutions obtained here cannot readily be obtained through other methods. Section IV deals with general properties of a mixed crystal. Explicit calculations are represented for the properties of the DOS of several specific systems in Sec. V. Both fixed-end and cyclic-boundary conditions are used to determine the use of the Bloch theorem. By restricting them to the simplest cases, these results may be compared with a more straightforward calculation using Bloch properties without standing waves. Further study on more complicated systems shall be reported in a later work.

II. BASIC FORMULATION

Dynamic equations of the two-dimensional harmonic lattice can often be approximated by nearest-neighbor interactions.[6] Specifically, we shall consider a two-dimensional rectangular lattice composed of $N\times M$ particles located at the integer points (n,m), $1\le n\le N$, $1\le m\le M$. The in-plane vibration may be separated into independent motions in m and n directions. If a harmonic frequency ω is assumed, the equations of motion in either the n and m direction are the following:

$$-\omega^2 m_{n,m}v_{n,m}=K'_{n,m;n,m-1}(v_{n,m-1}-v_{n,m})+K'_{n,m;n,m+1}(v_{n,m+1}-v_{n,m})$$
$$+K_{n,m;n-1,m}(v_{n-1,m}-v_{n,m})+K_{n,m;n+1,m}(v_{n+1,m}-v_{n,m})\,, \tag{1}$$

$1\le n\le N$, $1\le m\le M$.

Defining the matrices

$$\underline{M}(n)_{j,k}=\delta_{j,k}m_{n,j} \tag{2}$$

and

$$\underline{K}'(n)=\begin{bmatrix} K'_{n,1;n,0}+K'_{n,1;n,2}+K_{n,1;n-1,1}+K_{n,1;n+1,1} & -K'_{n,1;n,2} & 0 \\ -K'_{n,2;n,1} & K'_{n,2;n,1}+K'_{n,2;n,3}+K_{n,2;n-1,2}+K_{n,2;n-1,2} & 0 \\ 0 & 0 & \ddots \end{bmatrix}, \tag{3}$$

with

$$\underline{K}(n)_{j,k}=\delta_{j,k}K_{n,j;n+1,j} , \tag{4}$$

we can rewrite Eq. (1) in matrix form:

$$[\underline{K}'(n)-\omega^2\underline{M}(n)]\vec{v}(n)=\underline{K}(n)\vec{v}(n+1)+\underline{K}^T(n-1)\vec{v}(n-1), \quad n=1,2,\ldots,N \tag{5}$$

where $\vec{v}(n)$ is a vector defined by

$$[\vec{v}(n)]_k=v_{n,k} . \tag{6}$$

We also impose the fixed-end boundary conditions

$$\vec{v}(0)=\vec{v}(N+1)=0 , \tag{7}$$

since

$$V_{0,m}=V_{N+1,m}=0 \text{ for any } m \text{ and } V_{n,0}=V_{n,M+1}=0 \text{ for any } n .$$

The characteristic equation is a huge $(N\times M)$ by $(N\times M)$ block-diagonal determinant,

$$\det||\underline{S}||=0 ,$$

with

$$\underline{S}(\omega^2)=\begin{bmatrix} \underline{K}'(1)-\omega^2\underline{M}(1) & \underline{K}(1) & 0 & \cdots \\ \underline{K}(1)^T & \underline{K}'(2)-\omega^2\underline{M}(2) & \underline{K}(2) & \cdots \\ \underline{0} & \underline{K}(2)^T & \vdots & \cdots \\ \vdots & \vdots & & \\ \cdots & \cdots & \cdots & \ddots \end{bmatrix} . \tag{8}$$

The above block-diagonal determinant is very cumbersome to analyze analytically. In order to proceed we shall follow the procedure of Ref. 1 and introduce

$$\underline{A}(n)=[\underline{K}(n)]^{-1}[\underline{K}'(n)-\omega^2\underline{M}(n)] . \tag{9}$$

Equation (5) is now in the form

$$\underline{A}(n)\vec{v}(n)=\vec{v}(n+1)+\vec{v}(n-1) , \quad n=1,\ldots,N \tag{10}$$

since $\underline{K}^T=\underline{K}$.

Depending on the structures of the species, the matrices $\underline{A}(n)$ can be quite different for different n's. For convenience, we shall consider one frequently occurring structure of $\underline{A}(n)$ as the host matrix $\underline{A}_H$ and the other $\underline{A}(n)$'s as impurity matrix $\underline{A}_I$. Thus $\underline{A}(1)=\underline{A}(2)=\cdots\underline{A}(n_1-1)=\underline{A}_H$, until at line site n_1 where $\underline{A}(n_1)=\underline{A}_I\neq\underline{A}_H$. The matrices $\underline{A}(n_1+1),\ldots$ return to $\underline{A}_H$ until another impurity line site $n=n_1+n_2$ is reached, where $\underline{A}(n_1+n_2)\neq\underline{A}_H$. In general, it is not necessary for the impurity matrices to be identical to each other. Analysis of Eq. (10) is analogous to the procedure in Ref. 1 for the linear systems.

We shall first diagonalize $\underline{A}_H$ through an orthogonal transformation $\underline{D}$, so that

$$\underline{D}\,\underline{A}\,\underline{D}^{-1}=\underline{A}_d , \tag{11}$$

with

$$(\underline{A}_d)_{j,k}=\delta_{j,k}a_j . \tag{12}$$

Let $\vec{u}(n)=\underline{D}\vec{v}(n)$; Eq. (10) becomes

$$\vec{u}(n+1)=\underline{A}_d(n)\vec{u}(n)-\vec{u}(n-1) . \tag{13}$$

Since $\vec{u}(0)=\vec{0}$, it is clear that every component of $\vec{u}(n)$ is in the form of a standing wave along the n direction as in the following:

$$u_j(n)=u_j^{(0)}(n)=C_j^{(0)}\sin(n\Phi_j), \quad n\leq n_1 \tag{14}$$

with

$$\Phi_j=\cos^{-1}(a_j/2) . \tag{15}$$

At the line site $n=n_1+1$, we get instead

$$\begin{aligned}\vec{u}(n_1+1)&=(\underline{A}_I-\underline{A}_H)\vec{u}(n_1)\\ &\quad+[\underline{A}_H\vec{u}(n_1)-\vec{u}(n_1-1)]\\ &=\underline{\Delta}\vec{u}(n_1)+\vec{u}^{(0)}(n_1+1) ,\end{aligned} \tag{16}$$

where

$$\underline{\Delta}=\underline{D}(\underline{A}_I-\underline{A}_H)\underline{D}^{-1} . \tag{17}$$

It is important to realize at this point that Eq. (16)

represents interferences between the original undisturbed set of standing waves $\vec{u}^{(0)}(n)$ and a new set of standing waves $\vec{u}\,'(n)$ generated by the deviation of $\underline{A}_I$ from $\underline{A}_H$. The net effect can be reexpressed as a new set of standing waves differing both in magnitudes and phases from the original $u^{(0)}(n_1+1)$. More specifically,

$$\vec{u}(n_1+1)=\vec{u}\,'(n_1+1)+\vec{u}^{(0)}(n_1+1)\ , \tag{18}$$

where

$$\vec{u}\,'_j(n_1+1)=\left[\sum_k \Delta_{jk}C_k^{(0)}\sin(n_1\Phi_k)\frac{1}{\sin\Phi_j}\right]\times\sin\Phi_j\equiv\alpha_j^{(0)}\sin\Phi_j\ .$$

Using the $\vec{u}^{(0)}(n+1)$ expression explicitly with

$$\begin{aligned}\vec{u}_j^{(0)}(n_1+1)&=C_j^{(0)}\sin(n_1+1)\Phi_j\\&=C_j^{(0)}\sin(n_1\Phi_j)\cos\Phi_j\\&\quad+C_j^{(0)}\cos(n_1\Phi)\sin\Phi_j\end{aligned}$$

in Eq. (17), we get

$$\begin{aligned}\vec{u}_j(n_1+1)&=[\alpha_j^{(0)}+C_j^{(0)}\cos(n_1\Phi)]\sin\Phi_j\\&\quad+C_j^{(0)}\sin(n_1\Phi_j)\cos\Phi_j\\&=C_j^{(1)}\sin(\Phi_j+\Psi_j^{(1)})\ ,\end{aligned} \tag{19}$$

where

$$\tan\Psi_j^{(1)}=C_j^{(0)}\sin(n_1\Phi_j)\times[\alpha_j^{(0)}+C_j^{(0)}\cos(n_1\Phi_j)]^{-1}$$

and

$$C_j^{(1)}\sin\Psi_j^{(1)}=C_j^{(0)}\sin(n_1\Phi_j)\ . \tag{20}$$

It is easy to see that for $s\le n$,

$$\begin{aligned}\vec{u}_j(n_1+s)&=\vec{u}_j^{(1)}(s)\\&=C_j^{(1)}\sin(s\Phi_j+\Psi_j^{(1)})\ .\end{aligned} \tag{21}$$

The same matching procedure, Eqs. (16)–(21), can be repeated at the new discontinuous site $n=n_1+n_2$. The only difference is that in $\vec{u}^{(1)}(n)$ an additional phase $\Psi_j^{(1)}$ is present. The resultant set of standing waves will then take the form

$$\begin{aligned}\vec{u}_j(n_1+n_2+s)&=\vec{u}_j^{(2)}(s)\\&=C_j^{(2)}\sin(s\Phi_j+\Psi_j^{(2)})\ ,\end{aligned} \tag{22}$$

with the matching condition being

$$\tan\Psi_j^{(2)}=C_j^{(1)}\sin(n_2\Phi_j+\Psi_j^{(1)})\times[\alpha_j^{(1)}+C_j^{(1)}\cos(n_2\Phi+\Psi_j^{(1)})]^{-1}\ , \tag{23}$$

$$C_j^{(2)}\sin(\Psi_j^{(2)})=C_j^{(1)}\sin(n_2\Phi_j+\Psi_j^{(1)})\ . \tag{24}$$

In general, the structures of $\underline{A}_n$ at the discontinuous line site can be different from site to site (see Fig. 1). (This is analogous to linear systems with more than two kinds of species.[10]) $(C_j^{(q-1)},\Psi_j^{(q-1)})$ can now be identified as the amplitude and phase of the jth component of $u^{(q)}(s)$ prior to a discontinuous line site, $n=n_1+n_2+\cdots+n_q$ and the $(C_j^{(q)},\Psi_j^{(q)})$ are the corresponding quantities after the wave propagates through this line.

In order to continue our analysis, it is most convenient to linearize Eqs. (23) and (24) in terms of $C_j^{(q)}\cos(\Psi_j^{(q)})$ and $C_j^{(q)}\sin(\Psi_j^{(q)})$, $j=1,\ldots,M$. Defining

$$\vec{x}_j(q)=C_j^{(q)}\cos(\Psi_j^{(q)}),\quad q=0,1,\ldots,0 \tag{25a}$$

and

$$\vec{y}_j(q)=C_j^{(q)}\sin(\Psi_j^{(q)})\ , \tag{25b}$$

we get

$$\begin{bmatrix}\vec{x}(q)\\ \vec{y}(q)\end{bmatrix}=\begin{bmatrix}\underline{1} & \underline{\beta}(q)\\ 0 & \underline{1}\end{bmatrix}\begin{bmatrix}\underline{C}(q) & -\underline{S}(q)\\ \underline{S}(q) & \underline{C}(q)\end{bmatrix}\times\begin{bmatrix}\vec{x}(q-1)\\ \vec{y}(q-1)\end{bmatrix}\ , \tag{26}$$

where

$$\begin{aligned}\underline{\beta}_{j,k}(q)&=\frac{1}{\sin\phi_j}\underline{\Delta}_{j,k}(q)\\&=\frac{1}{\sin\phi_j}[\underline{D}(\underline{A}_I-\underline{A}_H)\underline{D}^T]_{j,k}\ ,\end{aligned} \tag{27a}$$

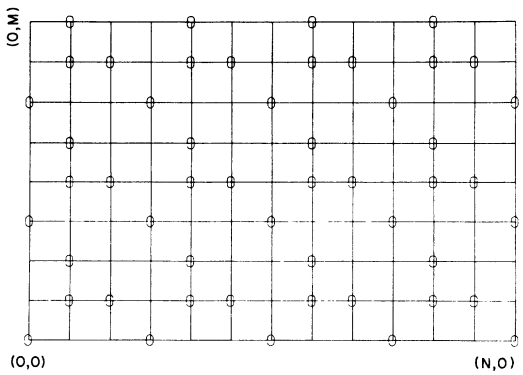

FIG. 1. Two-dimensional lattice; lattice sites without marks are occupied by an atom with mass M_A. Lattice sites with marks are occupied by an atom with mass M_B.

$$\underline{C}_{j,k}(q)=\delta_{j,k}\cos(N_q\phi_j)\ , \tag{27b}$$

$$\underline{S}_{j,k}(q)=\delta_{j,k}\sin(N_q\phi_j)\ . \tag{27c}$$

Stated in terms of the $\vec{X}_j(q)$ and $\vec{y}_j(q)$, the fixed-end boundary conditions become

$$\vec{y}(Q)=\vec{y}(0)=\vec{0}\ . \tag{28}$$

In order to understand the underlying implications of the above equations, we shall first study a few relatively simple examples in the following section. This enables us to demonstrate the general approach without going into the full generality.

III. EXPLICIT SOLUTIONS ON SIMPLE EXAMPLES

A. Reduced formulation

The general formulation in the preceding section is rather tedious. Emphasis on the indices tends to obscure the underline structure of the equations. We shall therefore restrict ourselves in this section to a class of two-dimensional systems. In this system only one kind of impurity line structure is repeated along the n direction. The periodic structure in the m direction need not be restricted. In this case all the $\underline{\beta},\underline{C},\underline{S}$ matrices in Eq. (27) are identical. Several transformations are now in order. First, let

$$\vec{y}\,'(q+1)=\underline{S}^{-1}\vec{y}(q)\ ,$$

$$\begin{bmatrix}\vec{x}(q+1)\\ \vec{y}\,'(q+1)\end{bmatrix}=\begin{bmatrix}\underline{C}+\underline{\beta}\underline{S} & -\underline{S}^2+\underline{\beta}\underline{C}\underline{S}\\ \underline{1} & \underline{S}^{-1}\underline{C}\underline{S}\end{bmatrix}\begin{bmatrix}\vec{x}(q)\\ \vec{y}\,'(q)\end{bmatrix}\ .$$

Since

$$\underline{S}\,\underline{C}=\underline{C}\,\underline{S}\ ,$$

we may then introduce

$$\underline{\lambda}=\underline{\beta}\underline{S} \tag{29}$$

and get

$$\begin{bmatrix}\vec{x}(q+1)\\ \vec{y}\,'(q+1)\end{bmatrix}=\begin{bmatrix}\underline{C}+\underline{\lambda} & \underline{\lambda}\,\underline{C}+\underline{C}^2-\underline{1}\\ \underline{1} & \underline{C}\end{bmatrix}\begin{bmatrix}\vec{x}(q)\\ \vec{y}\,'(q)\end{bmatrix}\ .$$

If we now introduce $\vec{x}\,'(q)=\vec{x}(q)+\underline{C}\vec{y}\,'(q)$, Eq. (26) is in the form

$$\begin{bmatrix}\vec{x}\,'(q+1)\\ \vec{y}\,'(q+1)\end{bmatrix}=\underline{T}\begin{bmatrix}\vec{x}\,'(q)\\ \vec{y}\,'(q)\end{bmatrix}\ , \tag{30}$$

where

$$\underline{\mu}=2\underline{C}+\underline{\lambda}=2\underline{C}+\underline{\beta}\underline{S}\ ,\qquad \underline{T}=\begin{bmatrix}\underline{\mu} & -\underline{1}\\ \underline{1} & \underline{0}\end{bmatrix}\ . \tag{31}$$

The fixed-end boundary conditions now become

$$\vec{y}\,'(Q)=\vec{y}\,'(0)=\vec{0}\ , \tag{28'}$$

leading to

$$\vec{y}\,'(Q)=(\underline{T}^Q)_{21}\vec{x}\,'(0)=0\ . \tag{32}$$

Thus the characteristic eigenvalue equation is expressed as

$$\det|\,(\underline{T}^Q)_{21}\,|=0\ . \tag{33}$$

Equation (33) is considerably simpler than the overall characteristic equation of Eq. (8). Since the detailed structure along the impurity line site is not specified, Eq. (33) still contains in itself a large class of interesting two-dimensional systems with periodic structures. The only remaining question is how to evaluate the off-diagonal submatrices $(\underline{T}^Q)_{21}$.

First, within the matrix $\underline{T}$, all submatrices commute to each other. Matrix products can therefore be evaluated as if $\underline{\mu}$ in Eq. (33) were scalar, and can be factored in exactly the same manner as that of the corresponding equations of the linear chains. In the latter case, the characteristic equations are known to be

$$\mu=\mu_q\equiv 2\cos\left[\frac{q\pi}{Q}\right],\quad q=0,\ldots,Q-1\ . \tag{34}$$

Equation (33) can therefore be factored as

$$\sum_{q=0}^{Q-1}(\underline{\mu}-\underline{\mu}_q\underline{1})\vec{x}\,'(0)=0\ , \tag{35}$$

i.e.,

$$\det|\,\underline{\mu}-\underline{\mu}_q\underline{1}\,|=0,\quad q=0,\ldots,Q-1\ . \tag{36}$$

The complicated characteristic equation [Eq. (8)] (which is a $N\times M$ degree polynomial in ω^2) is now factored into polynomials of order $N_0\times M$, $N_0=N/Q$.

To analyze further the contents of Eq. (35), it is necessary to use the explicit expressions for the eigenvalues and eigenamplitudes of the host line site. In the following, three typical numerical solutions are given.

B. Numerical solutions of a simple mixed grid

In this example we shall study the situation corresponding to Fig. 2. Here at the host line sites all atoms are the same, while at the impurity line sites a second kind of atom is located periodically, i.e.,

$$M_{1,k}=\begin{cases} M_B, & 1=\text{integer}\times N_0, \quad k=\text{integer}\times M_0 \\ M_A & \text{otherwise}. \end{cases} \tag{37}$$

Note that we can always reverse the order of treatment of N and M. Thus the characteristic equation (8) can also be factored into polynomials of ω^2 of order $N\times M_0$. Together this implies that Eq. (8) can be factored into polynomials of order $N_0\times M_0$ (the number of atoms in the unit cell). This is a pleasant surprise. The factorization is achieved for finite crystals, where the Bloch-type argument cannot be involved. As we shall see in the explicit evaluation, Eq. (33) indeed factors in this manner.

At the host line site, $\underline{A}_H$ can be diagonalized by eigenamplitudes of a homogeneous linear chain. The orthogonal transformation is

$$(\underline{D})_{j,1}=\left[\frac{1}{M_0P}\right]^{1/2}\sin\left[\frac{j1}{M_0P}\pi\right], \tag{38}$$

with the diagonal matrix elements of A_d being

$$a_l=2\cos\phi_l =\frac{1}{K}\left[2K'+2K-\omega^2 m_A-2K'\cos\frac{l\pi}{M_0P}\right]. \tag{39}$$

Substituting Eq. (38) into Eq. (17), we get

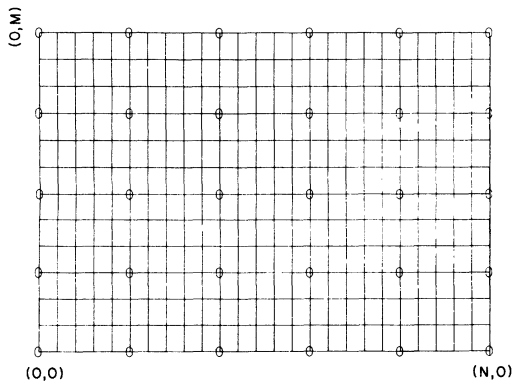

FIG. 2. Two-dimensional lattice; lattice sites without marks are occupied by an atom with mass M_A. Lattice sites with marks are occupied by an atom with mass M_B.

$$(\underline{\Delta})_{j,l}\equiv\Delta_{j,l} =\frac{2(M_A-M_B)\omega^2}{M_0PK}\sum_{p=1}^{P}\sin\left[\frac{p\pi}{P}j\right]\sin\left[\frac{p\pi}{P}l\right]. \tag{40}$$

This can be summed up explicitly. After some algebra, Eq. (40) becomes

$$\Delta_{j,l}=\frac{(M_A-M_B)\omega^2}{M_0PK}\times\left\{\frac{\sin\left[\frac{P-1}{2P}(j-l)\pi\right]}{\sin\left[\frac{1}{2P}(j-l)\pi\right]}\cos\left[\frac{j-l}{2}\pi\right]-(l\to -l)\right\}. \tag{41}$$

The following properties of $\Delta_{j,l}$ are obvious:

$$\Delta_{j,l}=\Delta_{l,j}, \tag{42a}$$

$$\Delta_{j,l}=0 \text{ if } j=\text{integer}\times P, \tag{42b}$$

$$\Delta_{j,l}=\Delta_{j,2P+l}, \tag{42c}$$

$$\Delta_{j,l}=-\Delta_{j,2P-l}, \tag{42d}$$

$$\Delta_{j,j}=\frac{(M_A-M_B)\omega^2}{M_0K}, \tag{42e}$$

$$\Delta_{j,l}=0 \text{ if } j-l=\text{odd integer}, \tag{42f}$$

and for $0<|j-l|<2P$, $j-l=$ even integer,

$$\frac{\sin\left[\frac{P-1}{2P}(j-1)\pi\right]}{\sin\left[\frac{1}{2P}(j-l)\pi\right]}\cos\left[\frac{j-l}{2}\pi\right]=-1.$$

Thus

$$\Delta_{j,l}=0 \text{ if } 0<|j-l|<2P. \tag{42g}$$

The above properties can be summarized easily with a rearrangement of the index j (and l) in the order

$$j \equiv \zeta(p) \equiv (p, 2P-p, 2P+p, \ldots, 2\zeta P-p, 2\zeta P+p, \ldots,), \quad 1 \le p \le P \tag{43}$$

so that j is of the order

$$j = 1, 2P-1, 2P+1, \ldots, 2, 2P-1, 2P+1, \ldots, P, 2P, \ldots, M_0 P) \ .$$

$\underline{\Delta}$ can then be blocked among those j and l sharing the same p, so that

$$\Delta_{\zeta(p),\zeta'(p)} = E_{\zeta\zeta'}$$

$$= \begin{cases} (-1)^{\zeta+\zeta'} \dfrac{(M_A - M_B)\omega^2}{M_0 K}, & p \ne P \\ 0, & p = P \end{cases}$$

$$\Delta_{\zeta(p),\zeta'(p')} = 0 \ , \quad p \ne p' \tag{44a}$$

i.e.,

$$\underline{\Delta} = \begin{bmatrix} \underline{E} & \underline{0} & \underline{0} & \underline{0} \\ \underline{0} & \underline{E} & & \underline{0} \\ \vdots & & \ddots & \vdots \\ \underline{0} & \underline{0} & \cdots & \underline{0} \end{bmatrix} . \tag{44b}$$

To take advantage of this, we shall first rewrite Eq. (36) in the form

$$\det | \underline{\Sigma}(q) + \underline{\Delta} | = 0 \ , \tag{45}$$

where

$$\underline{\Sigma}(q) = \underline{s}(2\underline{C} - \mu_q \underline{1})\underline{S}^{-1} \ , \tag{46}$$

with

$$(\underline{s})_{j,k} = \delta_{j,k} \sin\phi_j \ .$$

Since $\underline{\Sigma}(q)$ is a diagonal matrix, after rearranging its indices in the same manner as $\underline{\Delta}$, $\underline{\Sigma}(q)$ remains diagonal, i.e.,

$$\underline{\Sigma}(q) = \begin{bmatrix} \underline{H}(q, p=1) & \underline{0} & \cdots & \underline{0} \\ \underline{0} & \underline{H}(q, p=2) & \cdots & \underline{0} \\ \vdots & \cdots & \ddots & \vdots \\ \underline{0} & \underline{0} & \cdots & \underline{H}(q, p=P) \end{bmatrix} . \tag{47}$$

Equation (36) is now reduced to

$$\det | \underline{H}(q, P) | = 0 \tag{48}$$

and

$$\det | \underline{H}(q, p \ne P) + \underline{E} | = 0 \ , \quad p = 1, \ldots, P-1, \ q = 0, \ldots, Q-1. \tag{49}$$

The solution of Eq. (48) is

$$\phi_M = \frac{n}{N}\pi, \quad n = 0, 1, \ldots, N-1 \ . \tag{50}$$

In terms of ω^2, we get

$$\frac{1}{K}\left[2K' + 2K - \omega^2 M_A - 2K' \cos\left[\frac{M}{M_0}\pi\right]\right] = 2\cos\phi_M = 2\cos\frac{n}{N}\pi \ ,$$

i.e.,

$$\omega^2 M_A = 2K'\left[1 - \cos\frac{m}{M_0}\pi\right] + 2K\left[1 - \cos\frac{n}{N}\pi\right] \ ,$$

with

$$0 < M \le M_0 - 1, \quad 0 \le n \le N-1 \ . \tag{51}$$

For these types of solutions, a set of node lines passes through $m = M_0, 2M_2, \ldots$, where the second kind of atom is located. These solutions are therefore identical to those of the corresponding homogeneous lattice.

Since the specific order between N and M should not be important, Eq. (1) can be treated as M lattice lines each of length N. Equation (51) implies that there is another set of solutions where the node lines pass through $n = N_0, 2N_0, \ldots$, with the eigenvalues, so that

$$\omega^2 M_A = 2K'\left[1 - \cos\frac{n}{N}\pi\right] + 2K\left[1 - \cos\frac{n}{N}\pi\right] \ ,$$

$$0 \le m \le M-1, \quad 0 < n < N_0 - 1 \ . \tag{52}$$

This set of eigensolutions is implicitly hidden in Eqs. (30) and (35). With $q=0$, we get $\lambda_0 = 2$. $(2\underline{C} - \lambda_0 \underline{1})_{l,l}$ and $(\underline{S})_{l,l'}$ can both vanish for a given n and 1. Equation (35) can then be satisfied. This requires

$$N_0 \phi_l = n\pi, \quad l, n \text{ any integer} \ ,$$

and Eq. (52) follows.

Other solutions of Eq. (47) depend on both M_A and M_B and are naturally more complicated. Since

$$\underline{E} = \frac{(M_A - M_B)\omega^2}{M_0 K} \begin{bmatrix} 1 & -1 & 1 & \cdots \\ -1 & 1 & -1 & \cdots \\ 1 & -1 & 1 & \cdots \\ \cdots & \cdots & \cdots & \cdots \end{bmatrix} , \tag{44'}$$

TABLE I. Numerical solution corresponding to Fig. 2 with $m_A/m_B=4$, $k'/k=0.05$ with $M_0=5$, $P=5$, $N_0=3$, $Q=4$, and $\omega^2=2.96$.

J	1	9	11	19	21
U_j[a]	−2.115	2.178	−2.227	2.578	−2.667

[a]Other U_j's are identical to zero.

the determinant can be evaluated explicitly as

$$\sum_{\xi}[H_{\xi(p),\xi(p)}(p,q)]^{-1}+\frac{M_0K}{(M_A-M_B)\omega^2}=0\ , \tag{53}$$

$$p=1,\ldots,P-1,\quad q=1,\ldots,Q-1\ .$$

Each of the terms $H^{-1}_{\xi(p),\xi(p)}$ is a ration between a polynomial of degree (N_0-1) and another polynomial of degree N_0; Eq. (52) is indeed a polynomial of $N_0\times M_0$ degree in ω^2. While $N_0\times M_0$ is the number of atoms in the unit cell, the order of the overall characteristic equation (8) is a polynomial of $N\times M$, the total number of atoms in the whole lattice. This possibility of factorization of the overall characteristic equation to lower-order polynomial equations (determined by the dimension of the unit cell) is not restricted only to the specific example worked out here.

As long as a structure is repeated along a specific direction, factorization can be expected through the phase analysis along that direction. Since factorization may be achieved in more than one direction independently, an overall reduction of the secular equation follows. Note that this argument does not invoke a Bloch-type argument, and is therefore applicable to both finite and infinite lattices.

To further illustrate the procedure, we present here a numerical solution corresponding to $m_A/m_B=4$ and $k'/k=0.05$ with $M_0=5$, $P=3$, $N_0=3$, and $Q=4$. The solution in Tables I and II belongs to a choice of $p=q=1$ in Eq. (53). Simple numerical search of this equation indicates a zero position at $\omega^2=2.96$. Equation (35) is then used to determine $\vec{x}'(0)$ and $\vec{x}(0)$ (given by Table I). A rotation $\underline{D}$ applied to $\vec{x}(0)$ leads to $\vec{v}(1)$. Since $\vec{v}(0)=0$, all $\vec{v}(n)$'s can be found iteratively using Eq. (5). Indeed, the value $\vec{v}(N+1)$ is found to be zero. Furthermore, our solution exhibits symmetry with respect to both middle axes along N and along M, although these symmetries are not explicitly built in our solution. Specific values of the eigenvector $V_{j,k}$ with $j\leq 12$ and $k\leq 6$ are listed in Table II. Thus a correct eigenvalue is established without solving the secular equation, which is a 180×180 determinant. Also, the eigenvector is obtained without inversing a 180×180 matrix. The solution we outlined here required very little memory storage and computing time.

In Tables III and IV we present a similar solution associated with a slightly different set of constants. $M_A/M_B=4.0$ and $k'/k=0.25$ with $p=1$ and $q=2$. Numerical searching indicates a solution of Eq. (35) at $\omega^2=3.60$. The corresponding eigenvector is similarly calculated. Again the vector $\vec{V}(N+1)$ is identical to zero. This eigenvector is antisymmetric with respect to the middle axis along the N direction, but symmetric with respect to the middle axis along the M direction. The amount of computing is about the same as that of the previous example.

TABLE II. Values of eigenvectors $V_{j,k}$ corresponding to Fig. 2 with $\omega^2=2.96$, $M_A=1.0$, $M_B=0.25$, $k'=0.05$, $k=1.0$, $M_0=5$, $P=5$, $N_0=3$, and $Q=4$.

K \ J[a]	1	2	3	4	5	6	7	8	9	10	11	12
1	−0.00	0.00	−0.03	0.13	−1.96	0.13	−0.03	−0.05	0.21	−3.16	0.21	−0.05
2	0.00	−0.00	0.02	−0.01	1.70	−0.01	0.02	0.03	−0.02	2.76	−0.02	0.03
3	0.00	−0.00	0.01	−0.20	0.46	−0.20	0.01	0.02	−0.33	0.74	−0.33	0.02
4	−0.00	0.00	−0.02	0.17	−1.06	0.17	−0.02	−0.04	0.27	−1.72	0.27	−0.03
5	−0.00	0.00	−0.00	0.11	0.46	0.11	0.0	−0.00	0.18	0.74	0.18	0.00
6	0.00	−0.00	0.02	−0.29	0.65	−0.29	0.01	0.03	−0.46	1.05	−0.46	0.02

[a]$V_{j,k}=V_{25-j,k}=V_{j,12-k}$.

C. Further example

In this example we shall present a numerical solution with a somewhat more complicated impurity line structure. The periodic structure is shown in Fig. 3. There

$$M_{j,k}=\begin{cases} M_B, & j=\text{integer}\times N_0,\quad k=\text{integer}\times M_0\pm 1 \\ M_A & \text{otherwise}\ . \end{cases} \tag{54}$$

The numerical solution given in Tables V and VI corresponds to a set of constants of $M_0=7$, $P=3$, $N_0=3$, and $Q=5$. Instead of discussing the properties of matrix $\underline{\Delta}$ of Eq. (40), we shall simply outline its numerical value. Under a similar relabeling of indices, $\underline{\Delta}$ is block diagonal.

In terms of the sequence

$$j=(1,17,7,11,13,5,9;\,2,16,8,10,14,4,20;\,3,15,9;18,16,12)\ , \tag{55}$$

$$\underline{\Delta}=\begin{bmatrix} \underline{E} & 0 & 0 & 0 \\ 0 & \underline{E} & 0 & 0 \\ 0 & 0 & \underline{E}' & 0 \\ 0 & 0 & 0 & \underline{E}' \end{bmatrix}\ , \tag{56}$$

where

$$(\underline{E})_{j,k}=e_{|j-k|+1}\ , \tag{57a}$$

$$\vec{e}=(2.00,1.85,1.25,0.45,-0.45,-1.25,-1.80)\ ,$$

and

$$E^{-1}=\begin{bmatrix} 0.8 & 1.36 & 1.69 \\ 1.36 & 2.44 & 3.05 \\ 1.69 & 3.05 & 3.80 \end{bmatrix}\ . \tag{57b}$$

Although Eq. (53) is no longer true, the eigenvalue equation

$$\det|\,\Sigma(q)+\underline{\Delta}\,|=0 \tag{46'}$$

can still be evaluated in a straightforward manner. For example, with $q=1$ a zero of the determinant of the first block occurs at $\omega^2=3.495$. The corresponding value of $\vec{x}(0)$ is given in Table V. Again the iteration relation of Eq. (5) leads to all the other $\vec{v}(n)$'s. Not only $\vec{v}(N+1)$ thus obtained is zero, $V_{j,k}$ is also symmetrical with respect to reflection along the middle line of the N and M axis.

IV. GENERAL SOLUTIONS

To consider a more general mixed two-dimensional crystal, we shall start with Eq. (26).

TABLE III. Numerical solution corresponding to Fig. 2 with $M_A/M_B=4$, $k'/k=0.25$ with $M_0=5$, $P=5$, $N_0=3$, $Q=4$, and $\omega^2=3.60$.

J	1	9	11	19	21
U_j[a]	0.580	1.746	−0.580	0.742	−1.607

[a]Other U_j's are identical to zero.

Since the impurity lines may occur at different intervals, and the line structure may also be changing, the matrices $\underline{\beta}(q)$, $\underline{C}(q)$, and $\underline{S}(q)$ are changing within one complicated unit cell. The same overall structure shall, however, repeat itself from cell to cell. First, it is convenient to symmetrize the matrix $\underline{\beta}(q)$ through a scaling transformation,

$$\begin{bmatrix} \vec{x}(q) \\ \vec{y}(q) \end{bmatrix}\rightarrow\begin{bmatrix} \underline{s}^{-1/2} & 0 \\ 0 & \underline{s}^{-1/2} \end{bmatrix}\begin{bmatrix} \vec{x}(q) \\ \vec{y}(q) \end{bmatrix}\ , \tag{58}$$

$$\underline{s}_{j,k}=(\sin\phi_j)\delta_{j,k}\ .$$

Then

$$\begin{bmatrix} \vec{x}(q) \\ \vec{y}(q) \end{bmatrix}=\underline{L}(q)\begin{bmatrix} \vec{x}(q-1) \\ \vec{y}(q-1) \end{bmatrix}\ , \tag{59}$$

with

$$\underline{L}(q)=\begin{bmatrix} \underline{1} & \underline{\delta}(q) \\ 0 & 1 \end{bmatrix}\begin{bmatrix} \underline{C}(q) & -\underline{S}(q) \\ \underline{S}(q) & \underline{C}(q) \end{bmatrix}\ . \tag{60}$$

where

$$\underline{\delta}(q)=\underline{s}^{-1/2}[\underline{D}(\underline{A}_I-\underline{A}_H)\underline{D}^T]\underline{s}^{-1/2}\ . \tag{61}$$

Instead of $\underline{\beta}$ in Eq. (27a), $\underline{\delta}$ is now symmetric, i.e.,

$$\underline{\delta}(q)^T=\underline{\delta}(q)\ .$$

Applying Eq. (59) repeatedly within a unit cell, we now get

$$\begin{bmatrix} \vec{x}(q=0) \\ \vec{y}(q=0) \end{bmatrix}_{(n+1)\text{th cell}}=\underline{F}\begin{bmatrix} \vec{x}(q=0) \\ \vec{y}(q=0) \end{bmatrix}_{n\text{th cell}}\ , \tag{62}$$

where

TABLE IV. Values of eigenvector $V_{j,k}$ corresponding to Fig. 2 with $\omega^2=3.60$, $M_A=1.0$, $M_B=0.25$, $k'=0.25$, $k=1.0$, $M_0=5$, $P=5$, $N_0=3$, and $Q=4$.

K \ j[a]	1	2	3	4	5	6	7	8	9	10	11	12
1	0.29	0.61	0.02	0.33	−1.10	0.51	0.40	0.63	0.49	−0.68	0.03	−0.36
2	−0.46	−0.74	−0.26	−0.09	0.98	−0.37	−0.72	−0.90	−0.52	0.61	0.23	0.29
3	0.40	0.37	0.46	−0.42	0.16	−0.17	0.69	0.65	0.14	0.10	−0.50	0.06
4	−0.06	0.13	−0.23	0.38	−0.58	0.34	−0.15	−0.01	0.18	−0.36	0.27	−0.22
5	−0.37	−0.43	−0.35	0.21	0.28	−0.02	−0.61	−0.65	−0.24	−0.18	0.36	0.05
6	0.56	0.52	0.66	−0.59	0.22	−0.24	0.98	0.92	0.20	0.14	−0.71	0.08

[a] $V_{j,k}=-V_{25-j,k}=V_{j,12-k}$.

$$\underline{F}=\underline{L}(N_0)\cdots\underline{L}(2)\underline{L}(1)\ . \tag{63}$$

At the boundary of the last cell,

$$\begin{bmatrix}\vec{x}(q=0)\\ \vec{y}(q=0)\end{bmatrix}_{(Q+1)\text{th cell}}=\underline{F}^Q\begin{bmatrix}\vec{x}(q=0)\\ \vec{y}(q=0)\end{bmatrix}_{\text{first cell}}\ . \tag{64}$$

The boundary condition equation (28) now takes the form

$$(\underline{F}^Q)_{2,1}\vec{x}(q=0)=0\ . \tag{65}$$

Usually $\underline{F}$ cannot be transformed into the specific block-diagonal form of Eq. (31). One is required to evaluate products of noncommuting matrices. Factorization such as Eq. (36) is extremely difficult and perhaps too much to anticipate. (A detailed study of the eigenvalue equation for linear systems with more than two species is planned to be reported elsewhere.[13] Since Eq. (65) addresses quite general two-dimensional mixed crystals, it is desirable to carry the analysis as far as we can. Indeed, Eq. (65) can be reduced considerably, thanks to the unique form of $\underline{F}$. As is discussed in the Appendix, the diagonalization matrix $\underline{E}$ of the transformation F satisfies

$$\underline{F}\,\underline{E}=\underline{E}\,\underline{F}_d\ , \tag{66}$$

with

$$\underline{F}_d=\begin{bmatrix}\underline{U} & 0\\ 0 & \underline{U}^{-1}\end{bmatrix}\ , \tag{67}$$

$\underline{U}$ being diagonal, and

$$\tilde{\underline{E}}\equiv\begin{bmatrix}0 & \underline{1}\\ -\underline{1} & 0\end{bmatrix}\underline{E}^T\begin{bmatrix}0 & -\underline{1}\\ \underline{1} & 0\end{bmatrix}=\underline{E}^{-1}\ . \tag{68}$$

In terms of Eq. (66), Eq. (65) becomes

$$[\underline{E}(\underline{F}_d)^Q\tilde{\underline{E}}]_{2,1}\vec{x}(0)=0\ . \tag{69}$$

Substituting the explicit form

$$\underline{E}=\begin{bmatrix}\underline{e}_{11} & \underline{e}_{12}\\ \underline{e}_{21} & \underline{e}_{22}\end{bmatrix} \tag{70}$$

into the above equation, we get

$$(\underline{U}^Q\underline{r}\,\underline{U}^Q-\underline{r})\underline{z}=0\ , \tag{71}$$

where

$$\underline{r}=\underline{e}_{22}^{-1}\underline{e}_{21} \tag{72}$$

and

$$\vec{z}=\underline{e}_{22}^T\vec{x}(0,\text{ first cell})\ . \tag{73}$$

The eigenvalue equation is now

$$\det|\,\underline{U}^Q\underline{r}\,\underline{U}^Q-\underline{r}\,|=0\ . \tag{74}$$

In most cases, the ratio matrix $\underline{r}$ itself may still be block diagonal. Equations (71)—(74) can then be further factored into matrices with reduced dimensions. The nonlinear scattering of the standing waves of Eqs. (23) and (24) are now fully equivalent to the linearized equation of Eqs. (71) and (74).

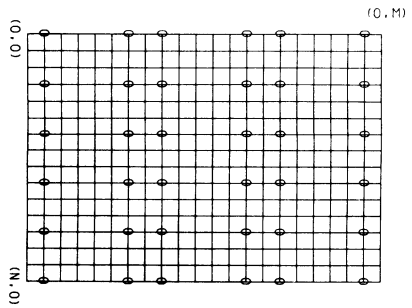

FIG. 3. Two-dimensional lattice; lattice sites without marks are occupied by an atom with mass M_A. Lattice sites with marks are occupied by an atom with mass M_B.

TABLE V. Numerical solution corresponding to Fig. 3 with $M_A/M_B=4$, $k'/k=0.25$, with $M_0=7$, $P=3$, $N_0=3$, $Q=5$, and $\omega^2=3.495$.

J	1	17	7	11	13	5	19
U_j[a]	−0.613	4.049	1.493	−0.740	0.985	4.799	−1.366

[a]Other U_j's are identical to zero.

V. DOS CALCULATIONS

A. Density of states of a double chain

In this section we shall discuss explicitly the limiting procedure leading to the DOS of a double chain. In this case, each atom is linked to its nearest neighbor in the same chain by a force constant k, and its nearest neighbor in the other chain by a force constant k'. One of the chains is populated with atoms $M_A=1$ only (homogeneous chain). The other chain is populated with M_A except for a periodic replacement of M_A by M_B at sites N_0, $2N_0$,... (cyclic chain). Equation (53) is now replaced by

$$\sum_{j=1}^{2}\left[\sin(\phi_j)\frac{2\cos(N_0\phi_j)-\mu_q}{\sin(N_0\phi_j)}\right]^{-1}\frac{1}{\eta}=0\ , \tag{75}$$

where

$$2\cos\phi_{1,2}=\frac{1}{k}(2k'+2k-\omega^2M_A\pm k')\ , \tag{76}$$

$$\eta=(M_A-M_B)\omega^2/(2k)\ , \tag{34'}$$

and

$$\mu_q=2\cos\frac{q\pi}{Q}\ .$$

This equation shall be obtained alternatively using the Bloch theorem in Sec. V B.

As Q tends to infinity, μ_q tends to a continuum. The DOS in terms of q and μ_q should be

$$G(\mu)d\mu=G(q)dq\ ,$$

i.e.,

$$G(\mu)=\frac{1}{\pi}\frac{2}{(4-\mu^2)^{1/2}}\Theta(4-\mu^2)\Theta(\mu)\ . \tag{77}$$

However, ω^2 is now a multivalued function of μ. With any given value of ω^2, there may be N_0 values of μ. The DOS therefore possesses N_0 components. A convenient procedure is to calculate μ in terms of ω^2 so that

$$\mu=\mu_j(\omega^2),\quad j=1,\ldots,N_0\ . \tag{78}$$

Since μ is always in the range $|\mu|\leq 2$, a given ω^2 may be in the band gap of some components. In terms of Eq. (79), the overall DOS can be calculated easily through

$$G(\omega^2)=\sum_j G(\mu_j)\left|\frac{d\mu_j}{d\omega^2}\right|\ . \tag{79}$$

In Fig. 4 we have plotted G corresponding to $N_0=2$. $M_B/M_A=0.5$ and $k'/k=0.1$. To understand the essential feature of this spectrum it is worthwhile to write down the explicit solutions of the individual uncoupled chains ($k'=0$). For the well-known homogeneous chain,

$$G_H(\omega^2)=\frac{1}{\pi}\frac{1}{[(4-\omega^2)\omega^2]^{1/2}}\Theta(\omega^2)\Theta(4-\omega^2)\ . \tag{80}$$

TABLE VI. Values of eigenvectors $V_{j,k}$ corresponding to Fig. 3 with $\omega^2=3.495$, $M_A=1.00$, $M_B=0.25$, $k'=0.25$, $k=1.00$, $M_0=7$, $P=3$, $N_0=3$, and $Q=5$.

K \ J[a]	1	2	3	4	5	6	7	8	9	10
1	2.013	0.722	2.055	−0.507	−1.898	−0.777	−2.034	1.236	−1.176	1.549
2	−2.184	−1.735	−2.099	0.465	2.210	1.756	1.909	−0.427	0.475	−1.634
3	0.595	2.076	0.352	0.016	−0.857	−2.001	−0.199	−1.406	1.219	0.368
4	1.073	−0.568	1.226	−0.355	−0.861	0.499	−1.381	1.572	−1.429	0.871
5	−1.521	−2.086	−1.342	0.246	1.678	2.065	1.056	0.544	−0.408	−1.096
6	0.962	3.359	0.569	0.026	−1.387	−3.237	−0.322	−2.276	1.973	0.595
7	−0.277	−1.640	−0.071	−0.067	0.505	1.585	−0.201	1.308	−1.135	−0.139

[a]$V_{j,k}=V_{21-j,k}=V_{j,15-k}$.

In our formulation it can be easily obtained by substituting $\mu=2\cos\phi$ into Eq. (79) or equivalently by

$$\mu=\mu_H(\omega^2)=\cos(2\phi)\ , \tag{81a}$$

where

$$\cos\phi=1-\omega^2/2\ . \tag{81b}$$

The spectrum of the alternative chain is also well known. This can be rederived with [1,3]

$$\mu=\mu_c(\omega^2)=-[2\cos(2\phi)+\beta\sin(2\phi)]$$
$$=-m'\omega^4+2(1+m')\omega^2-2\ , \tag{82}$$

leading to

$$G_C(\omega^2)=\frac{1}{\pi}\frac{2}{(4-\mu^2)^{1/2}}\left|\frac{d\mu}{d\omega^2}\right|\Theta(4-\mu^2)\Theta(\mu^2)$$
$$=\begin{cases}\dfrac{1}{\pi}\dfrac{4}{(4-\mu^2)^{1/2}}\,|1+m'-m'\omega^2|\ , & 0<\omega^2<2,\ \text{acoustic band or } 2/m'<\omega^2<2/m'+2,\ \text{optical band}\\ 0\quad\text{otherwise}\ . \end{cases} \tag{83}$$

When the coupling k' is present, individual eigenvalues are perturbed by the interaction. This changes the form of G_H and G_C. More specifically, μ_j can be evaluated from Eq. (79) with

$$\mu_\pm=a\pm(a^2-4b)^{1/2}\ , \tag{84}$$

where

$$a=\cos(2\phi_1)+\cos(2\phi_2)$$
$$+(\cos\phi_1+\cos\phi_2)\Delta\ ,$$
$$b=\cos(2\phi_1)\cos(2\phi_2)$$
$$+[\cos(2\phi_1)\cos\phi_2+\cos(2\phi_2)\cos\phi_1]\Delta\ ,$$
$$\Delta=\frac{1-m'}{2}\omega^2\ .$$

In examining Fig. 5, first we note the existence of the band gap at $\omega^2=0$, with its width roughly $2k'$. This can be readily understood. Usually two nearly degenerate eigenvalues repulse each other under interaction. At $\omega^2=0$, however, ω^2 cannot become negative. Thus both eigenvalues move to a larger ω^2 region. Physically, the standing wave of the homogeneous chain is incompatible with the standing waves of the cyclic chain in the long-wavelength limit. The linkage of k' makes it impossible for the double chain to satisfy its boundary conditions. Secondly, near the other band edge of the acoustic band ($\omega^2=2$), the interaction k' mixed part of the sharp rise of the DOS of the original acoustic band $G_C(\omega^2)$ to the homogeneous chain $G_H(\omega^2)$. A narrow band gap also developed near $\omega^2=2$. The spreading of the optical band into the shorter-wavelength region is expected. As can be seen, this spreading is again of the order $2k'$.

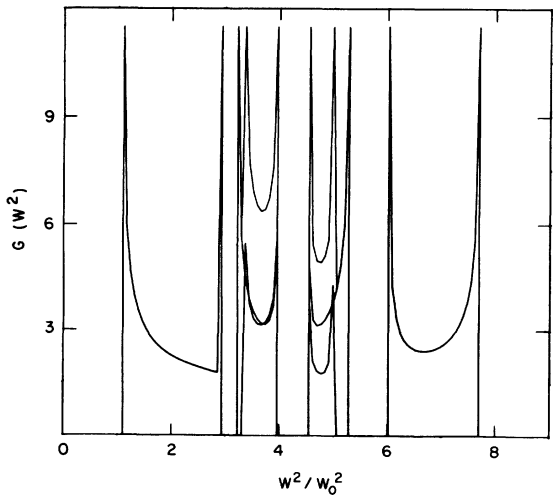

FIG. 4. DOS $G(\omega^2)$ of a double chain, see Eq. (79). The constants are $N_0=2$, $M_A=1$, $M_B=0.5$, and $k'=k=1$. DOS of each component is superimposed with the total DOS.

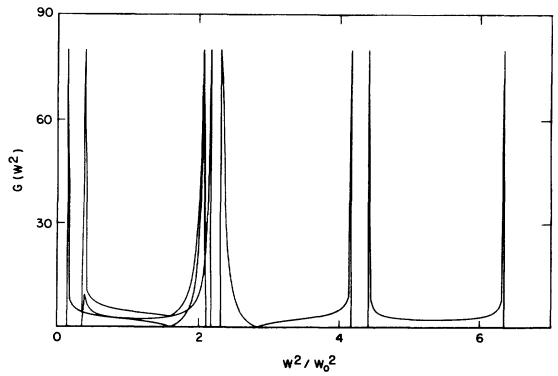

FIG. 5. DOS $G(\omega^2)$ of a double chain, see Eq. (79). The constants are $N_0=2$, $M_A=1$, $M_B=0.5$, $k'=0.1$, and $k=1$. DOS of each component is superimposed with the total DOS.

In the limit of small k', the above features may be realized approximated through perturbation expansion of Eq. (84). We then get

$$\mu_-(\omega^2)=(2-\omega^2+2k')^2-2+O(k'^2)$$
$$=\mu_H(\omega^2-2k')+O(k'^2)\ , \tag{85}$$

and similarly,

$$\mu_+(\omega^2)=\mu_C(\omega-2k')+O(k'^2)\ . \tag{86}$$

Therefore, in the region $\omega^2<2k'$, both $\mu_+(\omega^2)$ and $\mu_-(\omega^2)$ vanish up to the second order of k'.

It is also natural that a band gap should develop in the $\mu_-(\omega^2)$ component at $\omega^2=2$. With $\mu_-=\mu_H$, the divergence of $G(\mu_H)$ is canceled exactly by the zero in $|d\mu_H/d\omega^2|$, leading to smooth behavior of $G(\omega^2)$ at the middle of the band, $\omega^2=2$. The cancellation is not complete with μ_-, not exactly μ_H. A band gap arose in the region near $\omega^2=2$. In a sense, the springs k' attached to the homogeneous chain amount to a small added mass at alternative sites. The development of a small band gap in this region is therefore expected.

In Fig. 5 the spectrum of the DOS is plotted with $N_0=2$, $M_B/M_A=0.5$, and $k'/k=1.0$. Generally, the dependence is not very different from the earlier case. Properties such as the mixing of the different bands and the development of the band gap, particularly at $\omega^2=0$, is common to double chains with more complicated structures.

B. Density of states of cyclic strips

So far, we have always concentrated on finite lattices with a fixed boundary. As the size of a system increases, distribution of the eigenfrequencies becomes less sensitive to a particular choice of the boundary condition. A common DOS may be obtained with any type of boundary. One commonly used alternative is the cyclic condition. We shall therefore work out several examples demonstrating how such conditions are adapted in our formulation.

In order to satisfy the cyclic-boundary condition, Eqs. (28) and (65) are replaced by

$$(\underline{F}-\nu_q\underline{1})\begin{bmatrix}\vec{x}(q=0)\\ \vec{y}(q=0)\end{bmatrix}=0\ , \tag{87}$$

where

$$\nu_q=\exp(2\pi iq/Q),\quad q=0,1,\ldots,Q-1\ .$$

Naturally, the label identifying specific unit cells is no longer present. The simplest example corresponds to a strip with one single-segment structure repeating Q time before cycling. Equation (87) then reads

$$\begin{bmatrix}\underline{C}+\underline{\beta}\,\underline{S}-\nu_q\underline{1} & -\underline{S}+\underline{\beta}\,\underline{C}\\ \underline{S} & \underline{C}-\nu_q\underline{1}\end{bmatrix}\begin{bmatrix}\vec{x}\\ \vec{y}\end{bmatrix}=0\ .$$

Eliminating $\vec{x}$ in terms of $\vec{y}$, we get

$$[\underline{s}(2\underline{C}-\mu_q\underline{1})\underline{S}^{-1}+\underline{\beta}]\vec{y}=0\ , \tag{88}$$

where a real parameter $\mu_q=\frac{1}{2}(\nu_q+1/\nu_q)$ enters. For example, the previous example $\binom{BABA\cdots}{AAAA\cdots}$ of Sec. V A corresponds to

$$\underline{\beta}=\eta\begin{bmatrix}1 & 1\\ 1 & 1\end{bmatrix}\ ,$$

and the previous eigenvalue equation [Eq. (75)] can easily be rederived.

As a second example, we shall treat a slightly more complicated type of cyclic double chain with a two-segment structure. With the use of $\binom{A}{A}$ as the host and $\binom{B}{A}$ as the impurity, each segment is in the form $\binom{BAA\cdots B}{AAA\cdots B}$. The corresponding modulating matrix $\underline{F}=\underline{L}(2)\underline{L}(1)$ is more tedious. After a fair amount of algebra, Eq. (87) may be written as

$$c_1c_2-\eta(c_1s_2+c_2s_1)+\tfrac{1}{2}\eta^2(c_1s_{12}s_{22}+c_2s_{11}s_{21}+s_{11}s_{12}+s_{21}s_{22}+s_1s_2)+\tfrac{1}{4}\eta^2\mu_q(s_{11}s_{22}+s_{12}s_{21})=0\ , \tag{89}$$

where

$$c_j=\cos(n_1+n_2)\phi_j-\tfrac{1}{2}\mu_q\ ,$$
$$s_j=\sin(\eta_1+\eta_2)\phi_j/\sin\phi_j\ ,$$
$$s_{kj}=\sin n_k\phi_j/\sin\phi_j\ ,$$

with ϕ_j given by Eq. (76). Given a value μ_q, the above equation is a polynomial of ω^2 with degree $2(n_1+n_2)$. All branches of the DOS can be found when μ_q approaches a continuum. These density functions are somewhat more complicated than those explicitly demonstrated in Sec. V A. But the essential features are quite similar and need not be further discussed.

The general solution of Eq. (89) cannot be readily obtained by any traditional method. One might therefore evaluate a particular case with $n_1=1$ and $n_2=2$ corresponding to $\binom{BBAB\cdots}{BBAB}$. This is also a good example of a more complicated one-segment cyclic chain. With the identification of the host and

the impurity interchanged and $n=3$, Eq. (88) may also be used. Diagonalization of the host structure is now

$$\underline{R}=\frac{1}{\sqrt{2\gamma}}\begin{bmatrix}-\sqrt{\gamma+\eta} & \sqrt{\gamma-\eta}\\ \sqrt{\gamma-\eta} & \sqrt{\gamma+\eta}\end{bmatrix},$$

where $\gamma=(k^{12}+\eta^2)^{1/2}$. The rest of the algebra is straightforward, leading to an alternative expression exactly equivalent to Eq. (89). In either expression, the factorization of the secular equation is demonstrated explicitly. We shall not explicitly reexpress Eqs. (88) and (89) as polynomials in ω^2. Although rather tedious, both are identical to the solution obtained with a standard Bloch method. Obviously, in this case, it is just as easy to label every element and solve the secular equation directly. But Eqs. (88) and (89) already contain other situations not readily obtainable without a standing-wave formulation.

More specific discussions of other infinitely extended mixed crystals depend on direct extension of analysis in Sec. III. One also needs general solutions of one-dimensional mixed crystals with any structures, which we shall report in future papers.

VI. CONCLUSION

In this work we have analyzed the eigenvalues and eigenvectors of a class of finite and infinite two-dimensional mixed crystals. By generalizing a technique of phase analysis, the eigenvalues are obtained without explicitly solving the secular equation. Although the total number of atoms in the finite two-dimensional mixed crystals can be large, in our examples the eigenvalues are obtained through polynomial equations of the order equal to the total number of atoms in the unit cell. Since there is no need to store big matrices in the computer, and the systematic errors are reduced (because the overall secular equation is factorized analytically), numerical calculation is very fast and accurate. A traditional numerical evaluation of the eigenvectors of these examples is very time consuming and nearly impossible.

Generalization of the phase analysis to two-dimensional crystals with an arbitrary cell structure is very difficult. This is reflected in the noncommutating algebra of the modulating matrices. Nevertheless, the nonlinear coupling of phases can also be reduced to linear equations. With any given crystal structure, explicit analysis can be done to factorize the characteristic equations.

In the limit of infinite strips, both the fixed-end boundary condition and the cyclic-boundary condition lead to the same DOS. In some of our numerical examples of double strips, interesting properties common to strips of more complicated structures can be observed. These simple solutions can also be compared with the traditional extension of Bloch solutions without using the language of standing waves. Analysis on mixed two-dimensional infinite lattices can be further developed using explicit properties of the eigenvectors for one-dimension systems[13] and shall be represented in a planned future work. We are also currently working on a simultaneous diagonalization technique which would allow us to include symmetry properties along different directions more effectively.

ACKNOWLEDGMENTS

The author is grateful to Professor J. Thomson and Professor S. Georghiou for many stimulating discussions.

APPENDIX

The transformation matrices in Eq. (26) are unusual in the sense that they are not orthogonal transformations. Their specific forms call for a transformation defined in the following manner: Let

$$\underline{\Sigma}=\begin{bmatrix}\underline{\Sigma}_{11} & \underline{\Sigma}_{12}\\ \underline{\Sigma}_{21} & \underline{\Sigma}_{22}\end{bmatrix}, \tag{A1}$$

then

$$\tilde{\underline{\Sigma}}=\begin{bmatrix}\underline{\Sigma}_{22}^T & -\underline{\Sigma}_{12}^T\\ -\underline{\Sigma}_{21}^T & \underline{\Sigma}_{11}^T\end{bmatrix}, \tag{A2}$$

i.e.,

$$\tilde{\underline{\Sigma}}=\underline{R}\,\underline{\Sigma}^T\underline{R}^{-1},$$

with

$$\underline{R}=\begin{bmatrix}0 & \underline{1}\\ -\underline{1} & 0\end{bmatrix}, \tag{A3}$$

and $\underline{\Sigma}^T$ being the transpose of $\underline{\Sigma}$. As in the transpose transformation, when $\underline{\Sigma}=\underline{\Sigma}_2\underline{\Sigma}_1$,

$$\tilde{\underline{\Sigma}}=\tilde{\underline{\Sigma}}_2\tilde{\underline{\Sigma}}_2. \tag{A4}$$

Note that using this transformation for matrices in Eq. (60),

$$\begin{bmatrix}\underline{C} & -\underline{S}\\ \underline{S} & \underline{C}\end{bmatrix}\rightarrow\begin{bmatrix}\underline{C} & -\underline{S}\\ \underline{S} & \underline{C}\end{bmatrix}^{-1},$$

$$\begin{bmatrix}\underline{1} & \underline{\delta}\\ 0 & \underline{1}\end{bmatrix}\rightarrow\begin{bmatrix}\underline{1} & \underline{\delta}\\ 0 & \underline{1}\end{bmatrix}^{-1},$$

since all the submatrices are symmetrical. Thus

$$\tilde{\underline{L}}(j)=\underline{L}(j)^{-1}. \tag{A5}$$

By applying this transformation to product $\underline{F}$ of Eq. (63),

$$\tilde{\underline{F}}=\tilde{\underline{L}}(1)\cdots\tilde{\underline{L}}(N_0)=\underline{L}(1)^{-1}\cdots\underline{L}(N_0)^{-1}\ ,$$

i.e.,

$$\tilde{\underline{F}}=\underline{F}^{-1}\ . \tag{A6}$$

This in turn implies uncommon properties of the eigenvalues and eigenvectors. Let $\underline{E}$ be the diagonalization matrix, so that

$$\underline{F}\,\underline{E}=\underline{E}\,\underline{F}_d\ , \tag{A7}$$

where

$$\underline{F}=\begin{vmatrix}\underline{U} & 0\\ 0 & \underline{V}\end{vmatrix}\ , \tag{A8}$$

with diagonal $\underline{U}$ and $\underline{V}$. Transformation of Eq. (A7) then leads to

$$\tilde{\underline{E}}\,\underline{F}^{-1}=\tilde{\underline{F}}_d\tilde{\underline{E}}\ ,$$

i.e.,

$$\underline{F}\,\tilde{\underline{E}}^{-1}=\tilde{\underline{E}}^{-1}\tilde{\underline{F}}_d^{-1}\ , \tag{A9}$$

where

$$\tilde{\underline{F}}_d^{-1}=\begin{vmatrix}\underline{V}^{-1} & 0\\ 0 & \underline{U}^{-1}\end{vmatrix}\ .$$

Thus $\underline{U}^{-1}$ and $\underline{V}^{-1}$ can also be identified as the diagonalized submatrix of $\underline{F}$. Choosing the ordering of the eigenvalue properly, we may then arrange the eigenvectors (column vectors of $\underline{E}$) so that

$$\underline{V}=\underline{U}^{-1}\ . \tag{A10}$$

Equation (A9) now becomes

$$\underline{F}\,\tilde{\underline{E}}^{-1}=\tilde{\underline{E}}^{-1}\underline{F}_d\ . \tag{A11}$$

By comparing (A7) to (A11) it is obvious that we may also choose the normalization of individual column vectors of $\underline{E}$ and set

$$\tilde{\underline{E}}=\underline{E}^{-1}\ . \tag{A12}$$

In order to take advantage of the above relationships to the eigenvalue equation of Eq. (65), it is now necessary to write down explicitly

$$\underline{E}=\begin{bmatrix}\underline{e}_{11} & \underline{e}_{12}\\ \underline{e}_{21} & \underline{e}_{22}\end{bmatrix}\ , \tag{A13}$$

since

$$\underline{E}^{-1}=\begin{bmatrix}\underline{e}_{21}^{-1}\underline{G}^{-1} & -\underline{e}_{11}^{-1}\underline{H}^{-1}\\ -\underline{e}_{22}^{-1}\underline{G}^{-1} & \underline{e}_{12}^{-1}\underline{H}^{-1}\end{bmatrix}\ , \tag{A14}$$

with

$$\underline{G}=\underline{e}_{11}\underline{e}_{21}^{-1}-\underline{e}_{12}\underline{e}_{22}^{-1}\ ,$$

$$\underline{H}=\underline{e}_{22}\underline{e}_{12}^{-1}-\underline{e}_{21}\underline{e}_{11}^{-1}\ .$$

(A12) implies

$$\underline{e}_{21}^{-1}\underline{G}^{-1}=\underline{e}_{22}^{T}\ , \tag{A15a}$$

$$\underline{e}_{22}^{-1}\underline{G}^{-1}=\underline{e}_{21}^{T}\ . \tag{A15b}$$

Thus

$$\underline{G}^{-1}=\underline{e}_{21}\underline{e}_{22}^{T}=\underline{e}_{22}\underline{e}_{21}^{T}\ ,$$

so that $\underline{G}^{-1}$ is symmetrical, i.e.,

$$\underline{G}=\underline{G}^{T}\ . \tag{A16}$$

Similarly, $\underline{H}$ is also symmetrical. Substituting

$$\underline{L}=\underline{E}\,\underline{F}_d\tilde{\underline{E}} \tag{A7'}$$

into the eigenvalue equation [Eq. (65)], we now get

$$[\underline{E}(\underline{F}_d)^{Q}E]_{21}\vec{x}=0\ ,$$

i.e.,

$$(\underline{e}_{21}\underline{U}^{Q}\underline{e}_{22}^{T}-\underline{e}_{22}\underline{U}^{-Q}\underline{e}_{21}^{T})\vec{x}=0\ .$$

This can be rewritten as

$$(\underline{U}^{Q}\underline{r}\,\underline{U}^{Q}-\underline{r}^{T})\vec{z}=0\ , \tag{A17}$$

with

$$\underline{r}=\underline{e}_{22}^{-1}\underline{e}_{21} \tag{A18}$$

and

$$\vec{z}=\underline{e}_{22}^{T}\underline{e}_{21}\vec{x}\ .$$

Furthermore, using Eq. (A15a),

$$\underline{r}=\underline{e}_{21}^{T}\underline{G}\,\underline{e}_{21}\ ,$$

we find

$$\underline{r}^{T}=\underline{r}\ . \tag{A19}$$

Equation (A17) now takes the final form

$$(\underline{U}^{Q}\underline{r}\,\underline{U}^{Q}-\underline{r})\vec{z}=0\ . \tag{A20}$$

[1]C. C. Shih, Phys. Rev. B 23, 2797 (1981).
[2]E. W. Montroll, in *Proceedings of the Third Berkeley Symposium on Mathematical Statistics and Probability, Berkeley, 1955,* edited by Jerzy Neyman (University of California Press, Berkeley, 1955).
[3]L. Van Hove, Phys. Rev. 89, 1189 (1953).
[4]K. S. Dy, S. Y. Wu, and. T. Spratlin, Phys. Rev. 19, 4237 (1979).
[5]B. T. M. Willis and A. W. Pryor, *Thermal Vibrations in Crystallography* (Cambridge University Press, Cambridge, 1975), Vol. 67, p. 35.
[6]J. Hari, *Spectral Properties of Disordered Chain and Lattices* (Pergamon, New York, 1968), p. 15.
[7]P. Mazur, Phys. Rev. B 23, 6503 (1981).
[8]P. Dean and J. L. Martin, Proc. R. Soc. London 259, 409 (1961).
[9]P. Dean and M. D. Bacon, Proc. R. Soc. London 283, 64 (1965).
[10]Y. C. Chen, S. Y. Wu, and J. J. Sinai, Phys. Status Solidi B 104, 444 (1981).
[11]J. M. Narah, Math. Comput. 26, 859 (1972).
[12]C. C. Shih, J. Phys. C 13, L543 (1980); J. Phys. C 15, 5381 (1982).
[13]Chia C. Shih (unpublished).